Chemistry and Physics of Lipids 221 (2019) 1–7

Contents lists available at ScienceDirect

Chemistry and Physics of Lipids

journal homepage: www.elsevier.com/locate/chemphyslip

Effect of DMSO, urea and ethanol on hydration of stratum corneum model membrane based on short-chain length ceramide [AP]

N.Yu. Samoylova[a,b,*], M.A. Kiselev[a,c,d], T. Haußˢ[e]

[a] Frank Laboratory of Neutron Physics, Joint Institute for Nuclear Research, 141980, Dubna, Russia
[b] Skobeltsyn Institute of Nuclear Physics, Lomonosov Moscow State University, 119234, Moscow, Russia
[c] Lomonosov Moscow State University, 119234, Moscow, Russia
[d] Dubna State University, 141980, Dubna, Russia
[e] Macromolecular Crystallography, Helmholtz-Zentrum Berlin für Materialien und Energie, 14109, Berlin, Germany

ARTICLE INFO

Keywords:
Neutron diffraction
Stratum corneum
Lipid membrane
Ceramide [AP]
Hydration
Urea
Dimethyl sulfoxide
Ethanol

ABSTRACT

Hydration of oriented multilamellar membrane based on ceramide [AP] in the DMSO, urea and ethanol aqueous solutions at various solute concentrations was investigated by neutron diffraction. Neither urea nor DMSO influence the repeat distance of the membrane and internal structure of bilayer at their mole concentration of up to 0.15 and 0.10, respectively. The *d*-spacing reduction effect of both compounds was observed at their concentrations of 0.2 for urea and 0.2 and 0.4 for DMSO. Compared to hydration in the pure water, both urea and DMSO slow down the swelling process, and this slowdown is more pronounced with increasing in their concentration. At concentration of 0.2, urea and DMSO induce the slight phase separation of the fully hydrated samples; at the highest used concentration of 0.6, DMSO induces the strong time-depend separation of the sample probably due to fluidization of lipid bilayers. Ethanol at a used molar concentration of 0.03 leads to dissolution of the sample.

1. Introduction

The outermost layer of human epidermis, the *stratum corneum* (SC), provides the main barrier against water loss and against external chemical and microbiological influences. The SC consists of horny flattened cells (corneocytes), embedded in an extracellular lipid matrix containing predominantly ceramides, free fatty acids, cholesterol and a small fraction of cholesterol sulfate (Lampe et al., 1983; Elias, 1981). The unique composition and organization of SC lipid bilayers make the skin almost completely impermeable both for hydrophilic and lipophilic molecules (see review (van Smeden et al., 2014)). To facilitate the transport of substances such as drugs through skin, the chemical penetration enhancers (PEs) are applied in pharmaceutics. PEs affect the structure of SC, mainly lipid matrix, and can thus modulate the barrier properties of the skin. Dimethyl sulphoxide (DMSO), ethanol (EtOH) and urea are among the most commonly employed as PEs for transdermal drugs. The different mechanisms via which these PEs reduce the skin barrier function such as lipid fluidization, lipid extraction from SC, phase separation, increase in SC hydration, membrane defect formation etc. have been suggested in the past two decades (for reviews, see (Williams and Barry, 2004; Trommer and Neubert, 2006; Dragicevic and Maibach, 2015) and references herein).

Ethanol is well known to penetrate into skin and enhance the permeation of drugs (Kim et al., 1996). Ethanol was found to extract the lipids from SC, acting predominantly on free fatty acids (Kai et al., 1990; Bommannan et al., 1991; van der Merwe and Riviere, 2005; Kwak et al., 2012 and references herein) and induce the formation of water-permeable defects in the model membrane of skin (Thind et al., 2015) that may explain its action as a PE. Horita et al. found the alterations of the short periodicity phase of mouse SC lipids treated with EtOH-water mixture (Horita et al., 2015). However, earlier, Moghadem et al. reported that ethanol produces only very little change in lipid structure and hydrocarbon chain packing of human SC lipids (Moghadam et al., 2013). At physiological temperatures, no fluidization of lipid multilayers in the presence of ethanol neither in native skin samples (Krill et al., 1992) nor in model SC lipid mixtures (Kwak et al., 2012) was reported.

Previous studies suggested that the molecular mechanism of the transdermal transport enhancement caused by DMSO is consistent with its hydrogen bonding properties. At high concentration, DMSO limits the ceramide–ceramide interactions by forming the hydrogen bonds (further “H-bonds”) with the ceramide head groups (Notman et al.,

* Corresponding author. Current address: FLNP JINR, Joliot-Curie 6, 141980 Dubna, Russia.
E-mail address: rny03@nf.jinr.ru (N.Y. Samoylova).

https://doi.org/10.1016/j.chemphyslip.2019.02.012
Received 27 October 2018; Received in revised form 8 February 2019; Accepted 25 February 2019
Available online 27 February 2019
0009-3084/

2007) and/or alter the interfacial H-bond network involving the fatty acid molecules (Kwak and Lafleur, 2009), that consequently leads to the weakening of the lateral forces between the lipids, and to fluidization of the SC lipid bilayers. An alternative mechanism of the transdermal transport enhancement caused by DMSO is a transmembrane pore formation (Notman et al., 2008).

Urea has the oldest history of its application as PE. Penetration enhancing effect of urea for different substances is complex, depends on its concentration, composition of vehicle solvent, etc. (Williams, 2015). The mechanism, by which urea acts, is still unclear. Kim et al. suggested that urea forms hydrophilic diffusion channels within the skin barrier (Kim et al., 1993). Beastall et al. proposed that the action of urea is based on fluidization of SC lipids (Beastall et al., 1986). Recent NMR experiments have confirmed that urea influences the fluidity in both SC lipids and protein in intact SC (Pham et al., 2016). In contrast to that, no decrease of the lipid chain packing density of the model SC membranes in the 10% (w/w) aqueous urea solution and no change in the bilayer distance were recently observed (Mueller et al., 2016). Early, urea was reported to have no influence on membrane thickness of SC lipid mixtures at its concentrations of up to 30% at 32 °C; however, urea caused a concentration-depend shift in lipid phase transition (Zbytovská et al., 2009).

Previous researches have shown that simplified SC model membranes composed of short-chain ceramides (phytosphingosine-type ceramides [AP] and/or [NP]), fatty acid, cholesterol and cholesterol sulfate are suitable for studying the effects of permeation enhancers (Zbytovská et al., 2009; Engelbrecht et al., 2011, 2012; Ochalek et al., 2012a, b; Mueller et al., 2016; Čuříková et al., 2017). The lipids in the model membranes based on ceramide [AP] are arranged in a lamellar structure with periodicity of ~ 45–46 Å and exhibit extremely low hydration (Kiselev et al., 2005) that might be due to that the ceramide molecules are in a fully extended conformation as described by Kiselev (Kiselev, 2007). In this work we investigated the influence of DMSO, urea and ethanol on hydration kinetics of the oriented SC lipid membranes based on ceramide [AP].

2. Materials and methods

2.1. Sample preparation

N—(α—hydroxyoctadecanoyl)—phytosphingosine (CER [AP], purity of ~95%) was a gift from Cosmoferm (Delft, the Netherlands). Cholesterol (Ch, ≥99%), cholesterol sulfate (ChS, > 99%), palmitic acid (PA, ≥99%), stearic acid (SA, ≥98.5%), arachidic acid (AA, ≥99%), behenic acid (BA, ≥99%), lignoceric acid (LA, ≥99%) and cerotic acid (CA, ≥95%), deuterium oxide (D_2O, purity of ≥99.9 at.% D), deuterated urea-d4 (urea), deuterated ethanol-d6 (EtOH) and deuterated dimethyl sulfoxide-d6 (DMSO) were obtained from Sigma-Aldrich. Quartz plates were purchased from Spectrosil 2000, Saint-Gobain (Germany).

Several identical oriented samples of quaternary system CER[AP]/Ch/FFA/ChS (55/20/15/10 wt% or 1/0.7/0.46/0.22 in molar ratio) were prepared with free fatty acid composition (FFA) similar to that in the previously investigated membrane (Ryabova et al., 2010), i.e. PA/SA/AA/BA/LA/CA in the molar ratio of 1.3/3.3/6.7/41.7/36/6.7. Powder of each lipid was dissolved separately in chloroform/methanol (2/1 w/w) at a concentration of 10 mg/ml. Afterwards, the lipid solutions were mixed at the appropriate ratio. A mass of 1 g of the solution was spread over a 6.4 cm × 1.4 cm quartz plate. The samples were dried on a warm plate (≈ 40 °C) and were then stored in a vacuum desiccator at room temperature for 4 h to remove the rest of the solvent. To decrease mosaicity of samples and improve their scattering ability, samples were heated in a horizontal position at 80 °C during 20 min. After annealing, samples were gradually cooled down to room temperature and hydrated for 1–2 h with water vapour. Before measurements samples were stored at room conditions (≈ 20 °C, ≈ 40% relative humidity) during several (1–10) days.

2.2. Neutron diffraction experiment

Neutron diffraction experiments were carried out on the V1 membrane diffractometer of the research reactor of the Helmholtz-Zentrum Berlin für Materialien und Energie (HZB, Germany). Diffraction patterns were obtained by rocking the sample at fixed different angles of the two-dimensional position sensitive ^3He detector (20 × 20 cm^2 area, 1.5 × 1.5 mm spatial resolution) at neutron wavelength λ of 5.23 Å and sample-to-detector distance of 102.28 cm.

Experiments on hydration of oriented membranes were performed in excess of water-DMSO, water-urea and water-EtOH solution at molar fractions of solute (DMSO/urea/EtOH) X_{DMSO} = 0.1, 0.2, 0.4, 0.6, X_{urea} = 0.05, 0.1, 0.15, 0.2 and X_{EtOH} = 0.03. The quartz plate with a dry sample was introduced vertically into a chamber (Harroun et al., 2005) filled with excess of aqueous solution (EtOH, urea or DMSO at various concentrations in D_2O), and the first-order diffraction peak from the membrane was collected repeatedly for almost 7 h with the acquisition time of 10 min. During the next several hours four diffraction peak orders were collected one after another with the acquisition time of 10 min, ≈ 27 min, ≈ 27 min and ≈ 39 min, respectively. The fifth diffraction order was collected in the end of hydration with acquisition time of ≈ 98 min.

2.3. Data analysis

In measurements at the V1 diffractometer with a monochromatic neutron beam, diffraction patterns are recorded as a function of scattering angle 2θ and then are recalculated to a function of scattering vector $q = 2\pi Sin\theta/\lambda$. Diffraction pattern from multilamellar lipid membrane with repeat distance d contains a series of equidistant peaks at positions $q_h = 2\pi h/d$, where h is the order of diffraction peak.

The internal structure of membrane was derived from analysis of the neutron scattering length density (SLD) profile ρ(z) across the bilayer, calculated by Fourier transformation of the structure factors F_h according to Eq. (1) (Worcester and Franks, 1976; Schoenborn, 1976; Franks and Lieb,1979):

$$\rho(z) = a + b\sum_{h=1}^{h_{max}} \varphi_h \, |F_h| \cos\left(\frac{2\pi hz}{d}\right). \quad (1)$$

The absolute values of the structure factors $|F_h| = (I_h/L_hA_h)^{1/2}$ were calculated from the integrated peak intensities I_h and corrected for the Lorentz factor $L_h = 1/\sin 2\theta_h$ and the absorption coefficient A_h, which is calculated via (2)

$$A_h = \frac{\sin\theta_h}{2\mu l}\cdot\left[1 - \exp\left(-\frac{2\mu t}{\sin\theta_h}\right)\right]. \quad (2)$$

Assuming a lipid density of ~ 1 g/cm^3 at the weight of lipid material of 10 mg in an area of 8.96 cm^2, the thickness of the lipid film l was calculated to be ~ 11 μm. The linear attenuation coefficient μ was calculated in accordance with the chemical composition of the membrane, its packed density, the wavelength of neutron beam, and assuming a hydrated interbilayer spacing of ~ 1 Å (https://www.ncnr.nist.gov/instruments/bt1/neutron.html). For hydrated samples μ was calculated to be equal to 5.72 cm^{-1}. It varies extremely little with addition of DMSO, ethanol or urea and with change in their concentrations because the μ-values for these deuterated penetration enhancers are low and close to the μ-value for D_2O ($\mu_{d\text{-}DMSO}$ = 0.109 cm^{-1}, $\mu_{d\text{-}EtOH}$ = 0.072 cm^{-1}, $\mu_{d\text{-}urea}$ = 0.254 cm^{-1}, μ_{D2O} = 0.136 cm^{-1} versus μ-value for a dry SC membrane of 5.84 cm^{-1}). In our estimations, the largest absorption correction was ~ 0.9 for the first order diffraction peak (see Table S1 in Supplementary Materials).

The structure factor phase signs φ_h "−, +, −, +, −" for from the 1 st up to the 5th diffraction order were obtained in our previous work

(Kiselev et al., 2005). The coefficients a and b in Eq. (1) were determined from the procedure of SLD profile normalization using the values of neutron scattering length density of methyl and methylene groups: $SLD_{CH3} = -0.0085 \cdot 10^{-12}$ cm^{-2}, $SLD_{CH2} = -0.0031 \cdot 10^{-12}$ cm^{-2}.

The absolute error of the scattering length density profile was determined as an error of the indirect measurable parameters from the following equation:

$$\Delta\rho(z) = b \cdot \left[\sum_{h=1}^{h_{max}} (\Delta F_h)^2 \cos^2\left(\frac{2\pi h z}{d}\right) \right]^{1/2}. \quad (3)$$

The peak positions and their integrated intensities I_h were determined by Gaussian fitting using the OriginPro software package. The errors of structure factors ΔF_h were calculated taking into account counting statistics and background level.

3. Results and discussion

As previously established, the increase of the repeat distance of the 55%CER[AP]/20%Ch/15%FFA/10%ChS membrane with time due to its swelling in excess of pure D_2O (further considered as the "reference process" and the fully hydrated in D_2O membrane as the "reference state" when discuss the effect of urea, DMSO and ethanol on kinetics of membrane hydration) is described by exponential function (4)

$$d(t) = d_{fh} - \Delta d \cdot \exp(-t/\tau) \quad (4)$$

with characteristic time (τ) of 61 min and the repeat distance of the membrane in "fully hydrated state" $d_{fh} \approx 46$ Å (Ryabova et al., 2010). The Eq. (4) can be linearized:

$$Ln(d_{fh} - d) = Ln\Delta d - t/\tau. \quad (5)$$

The dependence of $Ln(d_{fh} - d)$ on time t is linear and yields the characteristic time τ (slope).

Fig. 1 presents a change in the membrane repeat distance (calculated from the position of the first diffraction peak) as a function of time during sample hydration in pure D_2O and at various concentration of urea/DMSO/EtOH. Fig. 2 shows the plots of the $Ln(d_{fh} - d)$ versus t which are no longer linear (except for the case of pure water). On these logarithmic dependencies, one can distinguish at least two linear segments for different time intervals. Therefore, to describe the kinetics of membrane swelling, the biexponential function (6) has been chosen:

$$d(t) = d_{fh} - \Delta d_1 \cdot \exp(-t/\tau_1) - \Delta d_2 \cdot \exp(-t/\tau_2). \quad (6)$$

As one can see in Fig. 1, the $d(t)$ dependencies are well described by Eq. (6). The calculated in the OriginPro software package characteristic times of swelling τ_1 and τ_2, the values of membrane repeat distance in fully hydrated state (d_{fh}), the parameters Δd_1 and Δd_2 as well as the goodness-of-fit parameters (coefficient of determination R^2 and reduced Chi^2) obtained from fitting of the $d(t)$ dependencies are summarized in Table 1. The values of Δd_1 and Δd_2 could be used to estimate the magnitude of a change in the membrane repeat distance during the hydration process or stages of the hydration process that occur with different (τ_1 or τ_2) characteristic times.

In general, the observed biexponential behaviour of the repeat distance may indicate that two parallel kinetic processes with different characteristic times ocurr in the system (for example, the processes of hydration at different levels of bonds „water-lipid"). However, a determination of the nature of biexponential behavior of $d(t)$ using only available neutron diffraction data without additional study is impossible.

3.1. Effect of urea on membrane hydration

The repeat distance of the membranes hydrated at low urea concentrations (X_{urea} = 0.05-0.15) decreases slightly compared to the reference sample hydrated in pure D_2O ($\approx$ 45.9 Å versus $\approx$ 46.0 Å).

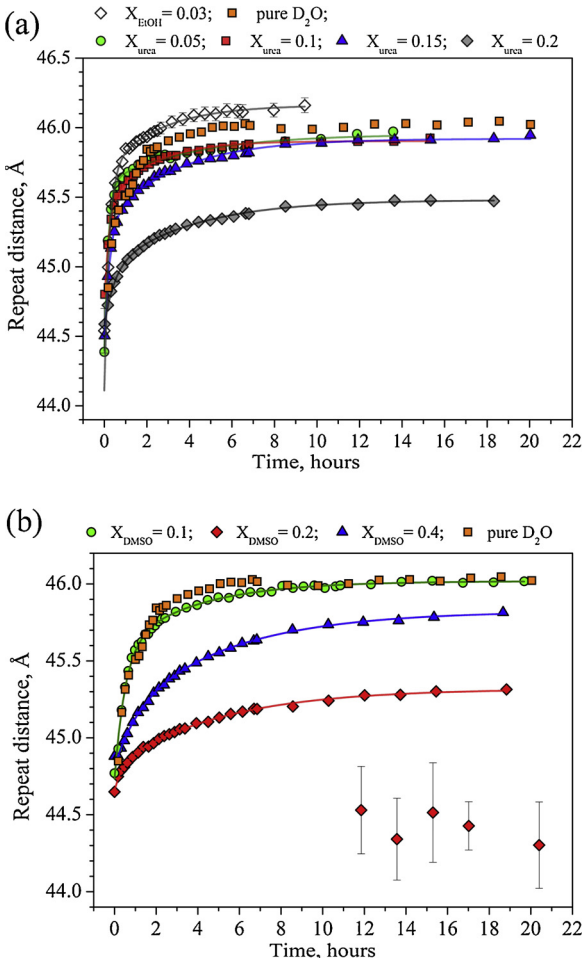

Fig. 1. Change of the repeat distance of the CER[AP]/Ch/FFA/ChS membranes during hydration in pure heavy water and at (a) X_{urea} = 0.05, 0.10, 0.15, 0.2 and X_{EtOH} = 0.03 and (b) X_{DMSO} = 0.1, 0.2, 0.4. Solid lines are fitting lines.

Increase in urea concentration up 0.2 leads to decrease in the value of membrane swelling by $\approx$ 0.4 Å (cf. d_{fh}-values in Table 1) and to increase in characteristic times of hydration process compared to hydration at lower urea concentrations.

NDPs measured from the samples at the end of hydration process are shown in Fig. 3. A left-side shoulder of the first diffraction peak at $\approx$ 0.11 Å^{-1} and a weak peak at 0.22 Å^{-1} on the NDPs of all samples hydrated with urea indicate a presence of a lamellar phase with repeat distance of 55.6 $\pm$ 0.6 Å. This phase is present initially in all dry samples. Previously, the phase with $d \approx 53$ Å was observed in the CER [AP]/Ch/FFA/ChS membranes with composition of 55/20/15/10 and 60/20/15/5 hydrated with water vapour at 57% related humidity and 20–32 °C and in water excess as well and was associated with a phase formed by pure long-chain behenic (C22:0) and lignoceric (C24:0) acids or with a phase enriched with these acids (Ryabova et al., 2010). Since the diffraction peaks of the phase enriched with long-chain FA do not overlap with the peaks from the main lamellar phase and thus cannot affect the calculated neutron SLD distribution for the main phase, we excluded this phase from further consideration.

NDPs from the samples hydrated at X_{urea} = 0.1, 0.15, 0.2, besides the peaks of the main phase with periodicity d_{fh} (see Table 1), show the right-side shoulders of the 3rd, 4th and 5th diffraction peaks from an additional lamellar phase (further "second phase") with periodicity of 44.5 $\pm$ 0.4 Å. The CER[AP]/Ch/FFA/ChS membranes with composition of 55/20/15/10 and 60/20/15/5 hydrated with water vapour were previously found to contain the similar minor phase with periodicity of 44.0–44.4 Å (Ryabova et al., 2010). For the samples at X_{urea} = 0.05 and

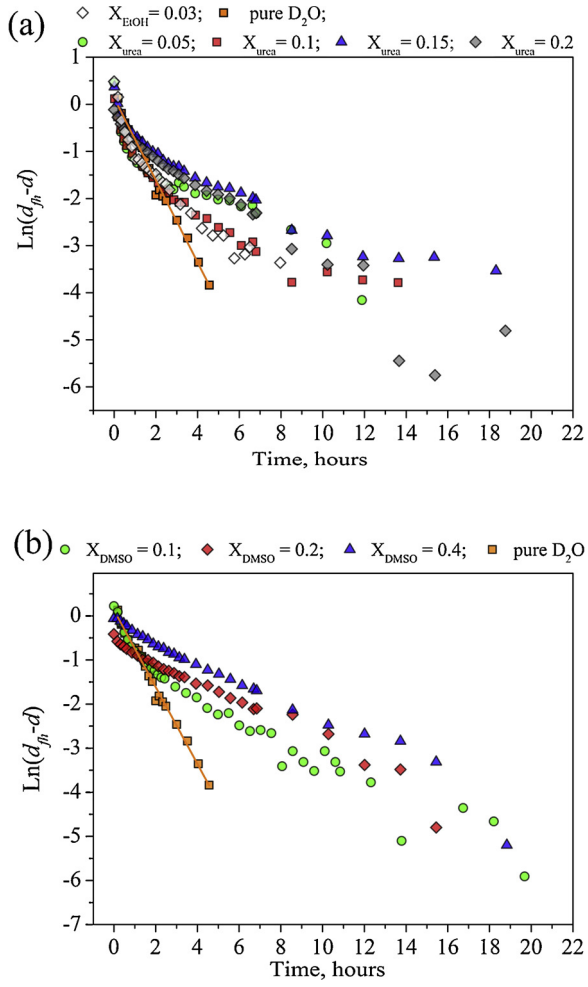

Fig. 2. Plot of $Ln(d_{fh} - d)$ versus time for the membrane hydration in pure heavy water and at (a) X_{urea} = 0.05, 0.10, 0.15, 0.2 and X_{EtOH} = 0.03 and (b) X_{DMSO} = 0.1, 0.2, 0.4. A straight line is a linear fit of the data for pure D_2O.

0.15 the diffraction peaks from the short-period phase have the intensities comparable with the level of the background noise that allows us to neglect this phase in calculation of neutron SLD distribution, considering the membranes as "near-one-phase systems". The phase

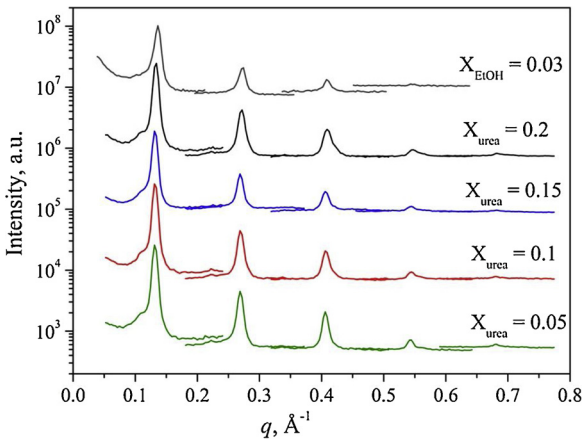

Fig. 3. Neutron diffraction patterns from the CER[AP]/Ch/FFA/ChS membranes measured after ≈ 13.5 h, 15.5 h, 20 h and 18.5 h from the beginning of hydration in heavy water at the urea concentration of X_{urea} = 0.05, 0.10, 0.15 and 0.2, respectively and after ≈ 8 h for the membrane hydrated at X_{EtOH} = 0.03.

separation in the samples at X_{urea} = 0.1, 0.2 is more pronounced: the intensities of the higher diffraction peaks of the second phase are comparable with intensities of the main phase, and we cannot longer consider the second phase as negligible. Moreover, due to the diffraction peaks from the main and second phases overlap and the resolution of NDP at low scattering vector values is limited, the individual contribution of structure factors of the different phases to the total integrated intensities of peaks cannot be resolved; therefore, a calculation of the neutron SLD distributions for the sample hydrated at X_{urea} = 0.1 and 0.2 would be incorrect.

The neutron SLD distributions for the main phase of fully hydrated at X_{urea} = 0.05, 0.15 samples calculated in accordance with Eqs. (1) and (3) are presented in Fig. 4a. The SLD profiles of both samples almost completely coincide within the error Δρ and are similar to that previously obtained for partially hydrated samples (Ryabova et al., 2010). This indicates that more than 14-hours hydration with water-urea solution with urea concentration of up to 0.15 does not affect the internal structure of the model membrane. The phase separation observed in the samples has no systematic correlation with urea concentration.

Table 1
Parameters of hydration of CER[AP]/Ch/FFA/ChS membranes in heavy water at various concentrations of penetration enhancers.

PE concentration	Δ*d*, Å	d_{fh}, Å	τ, min	Δd_i, Å	R^2	Chi^2
pure D_2O^*	1.24 ± 0.02	45.99 ± 0.01	τ = 61 ± 2	–	–	–
X_{EtOH} = 0.03	1.62 ± 0.16	46.16 ± 0.04	τ_1 = 13 ± 1 τ_2 = 148 ± 39	Δd_1 = 1.57 ± 0.07 Δd_2 = 0.49 ± 0.04	0.9947	0.8487
X_{urea} = 0.05	1.53 ± 0.02	45.92 ± 0.02	τ_1 = 9.5 ± 0.5 τ_2 = 166 ± 27	Δd_1 = 1.16 ± 0.03 Δd_2 = 0.37 ± 0.02	0.9977	1.5520
X_{urea} = 0.1	1.10 ± 0.02	45.901 ± 0.004	τ_1 = 12.8 ± 0.5 τ_2 = 123 ± 5	Δd_1 = 0.68 ± 0.01 Δd_2 = 0.47 ± 0.01	0.9994	0.1490
X_{urea} = 0.15	1.41 ± 0.02	45.91 ± 0.01	τ_1 = 13.7 ± 0.8 τ_2 = 181 ± 11	Δd_1 = 0.63 ± 0.02 Δd_2 = 0.83 ± 0.02	0.9983	0.4720
X_{urea} = 0.2	0.89 ± 0.02	45.48 ± 0.01	τ_1 = 29 ± 2 τ_2 = 232 ± 13	Δd_1 = 0.37 ± 0.02 Δd_2 = 0.51 ± 0.01	0.9991	0.1828
X_{DMSO} = 0.1	1.24 ± 0.02	46.02 ± 0.01	τ_1 = 31 ± 2 τ_2 = 223 ± 35	Δd_1 = 0.84 ± 0.07 Δd_2 = 0.44 ± 0.04	0.9960	0.7675
X_{DMSO} = 0.2	0.67 ± 0.02	45.32 ± 0.01	τ_1 = 22.6 ± 3 τ_2 = 303 ± 16	Δd_1 = 0.16 ± 0.01 Δd_2 = 0.50 ± 0.01	0.9980	0.2572
X_{DMSO} = 0.4	0.94 ± 0.02**	45.82 ± 0.01	τ_1 = 62 ± 8 τ_2 = 305 ± 20	Δd_1 = 0.31 ± 0.03 Δd_2 = 0.71 ± 0.03	0.9995	0.1153
X_{DMSO} = 0.6	1.15 ± 0.03	46.00 ± 0.02	τ = 41 ± 4	–	0.9832	

$\Delta d = d_{fh} - d_{dry}$, where d_{dry} (value $d(t = 0)$ on Fig.1) is the repeat distance of the SC membrane measured at room conditions before hydration; * data from (Ryabova et al., 2010); ** here $\Delta d = d_{fh} - d(t = 10\,\text{min})$.

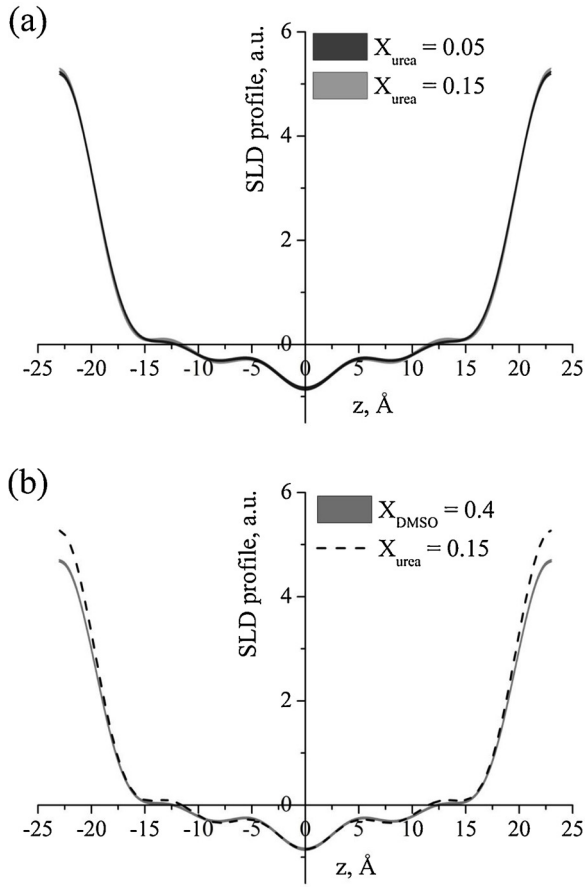

Fig. 4. Neutron scattering length density profile (ρ ± Δρ) of the CER[AP]/Ch/FFA/ChS samples hydrated (a) at X_{urea} = 0.05 (black shaded area) and X_{urea} = 0.15 (grey shaded area) and (b) at X_{DMSO} = 0.4 (grey shaded area) and X_{urea} = 0.15 (dash line).

3.2. Effect of ethanol on membrane hydration

NDP of the sample hydrated in the 1.5 M solution of ethanol (≈ 0.03 mole fraction of ethanol) displays a single-phase membrane (Fig. 3). After 2 h from the beginning of sample hydration the first structure factor begins to decrease monotonically, which is caused by sample dissolution (Fig. S1 in Supplementary materials). During ≈ 10 h the repeat distance of the membrane increases up to 46.16 Å that slightly exceeds the periodicity of the sample hydrated in pure heavy water. As in the case of hydration in the water-urea solution, the membrane swelling in water-EtOH solution is observed to occur in two stages: a fast initial stage and a subsequent slow one in accordance with Eq. (6) with characteristic times of 13 and 148 min.

The lipid film of the sample removed from the chamber after the experiment was partially washed away from the quartz plate. The fast dissolution of the sample may be perhaps related to the ability of ethanol to extract the lipids from the SC lipid matrix.

3.3. Effect of DMSO on membrane hydration

Figs. 1b and 5 present the $d(t)$ – dependencies for the samples in water-DMSO solutions at different DMSO concentrations. The NDPs from the fully hydrated samples are shown in Fig. 6. DMSO at 0.1 mole fraction has no influence on value of repeat distance. At X_{DMSO} = 0.2, the sample separates into two phases with repeat distances of 45.32 Å (main phase) and ≈ 44.4 Å (minor phase) in fully hydrated state. After 20 h hydration, the value of repeat distance of the main phase is considerably lower compared to the values of 46.0 and 45.8 Å for the

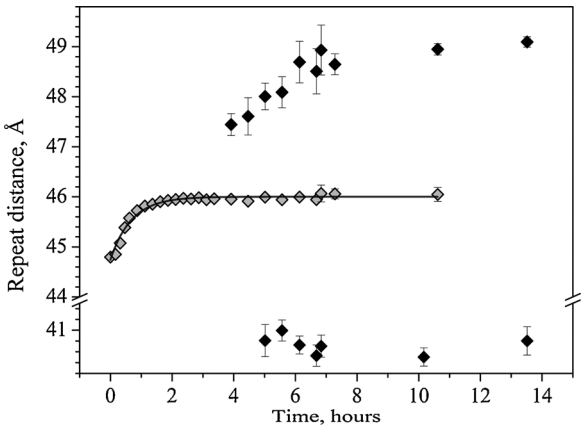

Fig. 5. Change of the repeat distance of the CER[AP]/Ch/FFA/ChS membrane during hydration in heavy water at X_{DMSO} = 0.6. The solid line is the fit by Eq. (4).

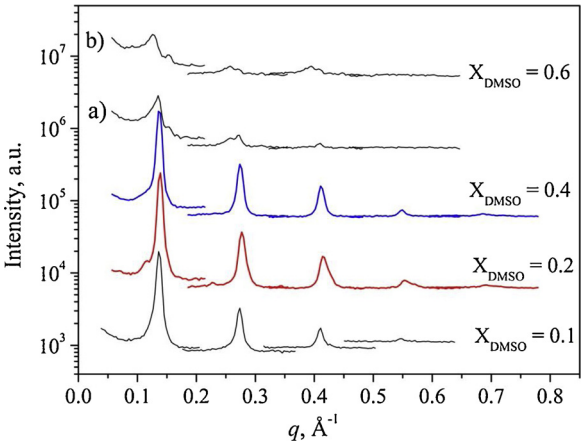

Fig. 6. Neutron diffraction patterns from the CER[AP]/Ch/FFA/ChS membranes measured at 20 °C after ≈ 18.5 h from the beginning of hydration in heavy water at X_{DMSO} = 0.1, 0.2, 0.4, and during time interval of (a) 410–464 min and (b) 610–703 min from the beginning of hydration at X_{DMSO} = 0.6.

sample at X_{DMSO} = 0.1 and 0.4, respectively (Table 1). Thus, a strong d-spacing reduction effect of DMSO is evident at its 0.2 mole fraction in water-DMSO solution: d = 45.32 Å versus 46.0 Å for reference state. Neutron SLD profile for the sample at X_{DMSO} = 0.4 (Fig. 4b) clear displays a decrease of the head-groups hydration compared to the sample hydrated at X_{urea} = 0.15.

Previously, the DMSO-induced dehydration of phospholipid membranes was observed in the X-ray and neutron scattering experiments with DPPC (Gordeliy et al., 1998; Kiselev et al., 1999; Cheng et al., 2015; Kiselev and Zemlyanaya, 2017), DMPC (Gorshkova and Gordeliy, 2007), PEs (Kinoshita et al., 2001) and DOPC (Cheng et al., 2015) membranes in excess of the water-DMSO solution. The drastic decrease in repeat distance of the phospholipid membranes, mostly at the low DMSO concentration (X_{DMSO} < 0.13), due to reduction of interbilayer distance (water layer thickness), was found to be attributed to a weakening of the repulsive hydration forces between the bilayers as a result of the DMSO-induced lipid surface dehydration by replacing of water molecules near lipid headgroups (Cheng et al., 2015; Schader et al., 2016).

DMSO at 0.6 mole fraction induces the membrane phase separation during hydration. The intensity of the initial phase becomes to decrease dramatically after 2 h from the beginning of hydration process (Fig. S2). Notable that this phase hydrates up to the d_{fh}-value of 46 Å much faster (τ = 41 min, Table 1) compared to hydration in pure water

(τ = 61 min). The second and third diffraction orders, which were begun to be recorded after ≈ 4 h from the beginning of hydration (Fig. 4), display an appearance of the phase with a longer periodicity that increases during hydration from 47.4 Å to 49.1 Å. The third phase with d of 40.8 ± 0.2 Å appears after 5 h from the beginning of hydration. These results are consistent with finding of molecular dynamics simulations of DMSO interaction with ceramide-2 bilayers, which have shown that DMSO molecules weaken the lateral forces between ceramides, that, at high concentration of DMSO (0.4 mole fraction and more), leads to a phase transition of lipid bilayers from gel to liquid crystalline phase (Notman et al., 2007). At X_{DMSO} = 0.6, in the DMSO-induced fluidized state of bilayers, the headgroups of lipids form more H-bonds with water molecules than in the gel state at $X_{DMSO} \leq 0.4$, that results in more rapid and significant swelling of initial lipid phase.

The slow membrane swelling in the presence of DMSO may be caused by features of interaction between DMSO and water which is well known. In aqueous solution, DMSO molecules form H-bonds with water which are stronger and have the longer lifetimes than water-water H-bonds, thereby increasing the solution viscosity (Luzar and Chandler, 1993). Indeed, with increasing DMSO concentration, solution viscosity η has a dramatic non-linear change: it first increases at X_{DMSO} of up to 0.35 and then again decreases (the reported η-values are 2.152, 3.455, 4.267, 3.398 mPa·s at 20 °C for X_{DMSO} = 0.1, 0.2, 0.4 and 0.6, respectively, versus 1.002 mPa·s for H_2O) (Schichman and Amey, 1971). Consequently, with increasing DMSO concentration up to X_{DMSO} = 0.4, solution diffusivity decreases that explains the slowdown of the sample hydration and increase in its characteristic times.

At the same concentrations of urea and DMSO, the retard of membrane swelling is less pronounced in urea solutions (cf. the characteristic times values in Table 1). The values for related viscosity of urea solution (η/η_{water}) at 25 °C extracted from the fit of the literature data summarized in (Halonen et al., 2017) are ~ 1.1, ~ 1.28, ~ 1.46 and ~ 1.85 for X_{urea} = 0.05, 0.1, 0.15 and 0.2, respectively. As one can see, these values are significantly lower than those for viscosity of DMSO solution at the same solute concentrations. Compared to DMSO-water H-bonds, the urea-water and urea-urea H-bonds are considerably weaker than those between water molecules and urea tends to form the specific urea-water clusters (Stumpe and Grubmüller, 2007]. However, in contrast to DMSO that is a single H-bond acceptor, urea whose molecule consists of two amine (–NH_2) groups (donors for 4 H-bonds) and the carbonyl (C═O) group (acceptor for one H-bond), can form more H-bonds with lipid headgroups, displacing hydrogen-bonded water molecules. The neutron SLD profiles for the samples at X_{urea} = 0.05 and 0.15 (Fig. 4a) show no difference between the internal structures of the membrane at these urea molar fractions in aqueous solution, indicating that urea does not penetrate into the bilayer in the concentration range investigated. This agrees with results obtained by Muller et al. in the recent study of CER[AP]/Chol/SA model membrane (Mueller et al., 2016) there no influence of urea on bilayer repeat distance and no additional water uptake in the head group region in the presence of 10 w% (≈ 3.4 mole %) urea in aqueous solution were observed. At X_{urea} = 0.2, the repeat distance of fully hydrated sample is only ≈ 45.5 Å that clear demonstrates a slight d-spacing reduction effect of urea. This finding is consistent with assumption that even at its 0.2 mole fraction urea does not incorporate into bilayer structure and is involved in H-bonds with lipids predominantly on the bilayer surface, preventing thus the water uptake. On the other hand, it was clear shown in (Pham et al., 2016) that urea has a tendency to fluidize the SC lipids, and the observed reduction of the membrane repeat distance at high urea concentration may result from a decrease in the thickness of lipid bilayer due to its transformation into liquid state.

4. Conclusion

Neutron diffraction measurements, using oriented multilamellar samples, have revealed that urea and DMSO, in the concentration range up to 0.2 and 0.4, respectively, influence the value and the rate of swelling of the short-period model membrane based on ceramide [AP]. Neither urea nor DMSO affect significantly the repeat distance of the membrane under hydration at their low concentrations (up to 0.15 and 0.1, respectively) in water solution. The d-spacing reduction effect of both compounds was revealed at their higher concentrations. No influence of urea on the bilayer internal structure was observed at its mole concentration up to 0.15. DMSO does not influence the lipid bilayer at low concentration, but at mole concentration of 0.6, it causes the strong phase separation of the membrane that is evidence of that at high concentrations, DMSO can reduce the skin barrier properties and enhance permeability by fluidizing the SC lipids.

The observed slowing down of the rate of membrane swelling with increasing of DMSO and urea concentration may be associated with the dynamic properties of the water-penetration enhancer solution, namely its viscosity, this is, however, requires the experimental verification using additional research methods.

Unlike DMSO and urea, ethanol already at 0.03 mole fraction leads to dissolution of the sample that made it impossible to study the membrane hydration at its higher concentrations.

Acknowledgments

This work was supported by the Russian Science Foundation (project number 14-12-00516). The authors would like to thank anonymous reviewers for their comments and corrections that helped to improve this paper.

References

Beastall, J., Guy, R.H., Hadgraft, J., Wilding, I., 1986. The influence of urea on percutaneous absorption. Pharm. Res. 3, 294–297.
Bommannan, B., Potts, R.O., Guy, R.H., 1991. Examination of the effect of ethanol on human stratum corneum in vivo using infrared spectroscopy. J. Control. Release 16 (3), 299–304.
Cheng, C.-Y., Song, J., Pas, J., Meijer, L.H.H., Han, S., 2015. DMSO induces dehydration near lipid membrane surfaces. Biophys. J. 109, 330–339.
Čuříková, B.A., Procházková, K., Filková, B., Diblíková, P., Svoboda, J., Kováčik, A., Vávrová, K., Zbytovská, J., 2017. Simplified stratum corneum model membranes for studying the effects of permeation enhancers. Int. J. Pharmaceut. 534, 287–296.
Percutaneous penetration enhancers chemical methods in penetration enhancement. In: Dragicevic, N., Maibach, H.I. (Eds.), Modification of the Stratum Corneum. Springer, Berlin.
Elias, P.M., 1981. Epidermal lipids, membranes, and keratinization. Int. J. Dermatol. 20, 1–19.
Engelbrecht, T.N., Schroeter, A., Hauß, T., Neubert, R.H.H., 2011. Lipophilic penetration enhancers and their impact to the bilayer structure of stratum corneum lipid model membranes: neutron diffraction studies based on the example Oleic Acid. Biochim. Biophys. Acta 1808, 2798–2806.
Engelbrecht, T.N., Deme, B., Dobner, B., Neubert, R.H.H., 2012. Study of influence of penetration enhancer isopropylmyristate on the nanostructure of stratum corneum lipid model membranes using neutron diffraction and deuterium labelling. Skin Pharmacol. Physiol. 25 (4), 200–207.
Franks, N.P., Lieb, W.R., 1979. The structure of lipid bilayers and the effects of general anaesthetics. J. Mol. Biol. 133, 469–500.
Gordeliy, V.I., Kiselev, M.A., Lesieur, P., Pole, A.V., Teixeira, J., 1998. Lipid membrane structure and interactions in dimethyl Sulfoxide/Water mixtures. Biophys. J. 75, 2343–2351.
Gorshkova, J.E., Gordeliy, V.I., 2007. Investigation of the interaction of dimethyl sulfoxide with lipid membranes by small-angle neutron scattering. Crystallogr. Rep. 52 (3), 535–539.
Halonen, S., Kangas, T., Haataja, M., Lassi, U., 2017. Urea-water-Solution properties: density, viscosity, and surface tension in an under-saturated solution. Emiss. Control Sci. Technol. 3, 161–170.
Harroun, T.A., Balai-Mood, K., Hauss, T., Otomo, T., Bradshaw, J.P., 2005. Neutron diffraction with an excess-water cell. J. Biolphys. 31, 207–218.
Horita, D., Hatta, I., Yoshimoto, M., Kita, Y., Todo, H., Sugibayashi, K., 2015. Molecular mechanisms of action of different concentrations of ethanol in water on ordered structures of intercellular lipids and soft keratin in the stratum corneum. Bioch. Bioph. Acta 1848, 1196–1202.
Kai, T., Mak, V.H.W., Potts, R.O., Guy, R.H., 1990. Mechanisms of percutaneous penetration enhancement: effect of n-alkanols on the permeability barrier of hairless mouse skin. J. Control. Release 12, 103–112.
Kim, C.K., Kim, J.J., Chi, S.C., Shim, C.K., 1993. Effect of fatty acids and urea on the penetration of ketoprofen through rat skin. Int. J. Pharm. 99, 109–118.
Kim, D.D., Kim, J.L., Chien, Y.W., 1996. Mutual hairless rat skin permeation-enhancing

effect of ethanol/water system and oleic acid. J. Pharm. Sci. 85 (11), 1191–1195.
Kinoshita, K., Li, S.J., Yamazaki, M., 2001. The mechanism of the stabilization of the hexagonal II (HII) phase in phosphatidylethanolamine membranes in the presence of low concentrations of dimethyl sulfoxide. Eur. Biophys. J. 30, 207–220.
Kiselev, M.A., 2007. Conformation of ceramide 6 molecules and chainflip transitions in the lipid matrix of the outermost layer of mammalian skin, the stratum corneum. Crystallogr. Rep. 54 (3), 549–553.
Kiselev, M.A., Lesieur, P., Kisselev, A.M., Grabielle-Madelmond, C., Ollivon, M., 1999. DMSO-induced dehydration of DPPC membranes studied by X-ray diffraction, small-angle neutron scattering, and calorimetry. J. Alloys. Compd. 286, 195–202.
Kiselev, M.A., Ryabova, N.Yu., Balagurov, A.M., Dante, S., Hauss, T., Zbytovska, J., Wartewig, S., Neubert, R.H., 2005. New insights into the structure and hydration of a stratum corneum lipid model membrane by neutron diffraction. Eur. Biophys. J. 34, 1030–1040.
Kiselev, M.A., Zemlyanaya, E.V., 2017. Dimethyl sulfoxide-induced dehydration of the intermembrane space of dipalmitoylphosphatidylcholine multilamellar vesicles: neutron and synchrotron diffraction study. Crystallogr. Rep. 62 (5), 763–767.
Krill, S.L., Knutson, K., Higuchi, W.I., 1992. Ethanol effects on the stratum corneum lipid phase behavior. BBABiomembranes 1112, 273–280.
Kwak, S., Lafleur, M., 2009. Effect of dimethyl sulfoxide on the phase behavior of model stratum corneum lipid mixtures. Chem. Phys. Lipids 161, 11–21.
Kwak, S., Brief, E., Langlais, D., Kitson, N., Lafleur, M., Thewalt, J., 2012. Ethanol perturbs lipid organization in models of stratum corneum membranes: an investigation combining differential scanning calorimetry, infrared and 2H NMR spectroscopy. Biochim. Biophys. Acta 1818, 1410–1419.
Lampe, M.A., Burlingame, A.L., Whitney, J., Williams, M.L., Brown, B.E., Roitman, E., Elias, P.M., 1983. Human stratum corneum lipids: characterization and regional variations. J. Lipid Res. 24, 120–130.
Luzar, A., Chandler, D., 1993. Structure and hydrogen bond dynamics of water–dimethyl sulfoxide mixtures by computer simulations. J. Chem. Phys. 98, 8160–8173.
Moghadam, S.H., Saliaj, E., Wettig, S.D., Dong, C., Ivanova, M.V., Huzil, J.T., Foldvari, M., 2013. Effect of chemical permeation enhancers on stratum corneum barrier lipid organizational structure and interferon alpha permeability. J. Mol. Pharm. Org. Process Res. 10, 2248–2260.
Mueller, J., Oliveira, J.S.L., Barker, R., Trapp, M., Schroeter, A., Brezesinski, G., Neubert, R.H.H., 2016. The effect of urea and taurine as hydrophilic penetration enhancers on stratum corneum lipid models. Biochim. Biophys. Acta 1858, 2006–2018.
Notman, R., den Otter, W.K., Noro, M.G., Briels, W.J., Anwar, J., 2007. The permeability enhancing mechanism of DMSO in ceramide bilayers simulated by molecular dynamics. Biophys. J. 93, 2056–2068.
Notman, R., Anwar, J., Briels, W.J., Noro, M.G., den Otter, W.K., 2008. Simulations of skin barrier function: free energies of hydrophobic and hydrophilic transmembrane pores in ceramide bilayers. Biophys. J. 95, 4763–4771.
Ochalek, M., Podhaisky, H., Ruettinger, H.H., Neubert, R.H.H., Wohlrab, J., 2012a. SC lipid model membranes designed for studying impact of ceramide species on drug diffusion and permeation, Part III: Influence of penetration enhancer on diffusion and permeation of model drugs. Int. J. Pharm. 436, 206–213.
Ochalek, M., Podhaisky, H., Ruettinger, H.H., Wohlrab, J., Neubert, R.H.H., 2012b. SC lipid model membranes designed for studying impact of ceramide species on drug diffusion and permeation − Part II: diffusion and permeation of model drugs. Eur. J. Pharm. Biopharm. 82, 360–366.
Pham, Q.D., Björklund, S., Engblom, J., Topgaard, D., Sparr, E., 2016. Chemical penetration enhancers in stratum corneum − Relation between molecular effects and barrier function. J. Control. Release 232, 175–187.
Ryabova, N.Yu., Kiselev, M.A., Dante, S., Hauss, T., Balagurov, A.M., 2010. Investigation of stratum corneum lipid model membranes with free fatty acid composition by neutron diffraction. Eur. Biophys. J. 39, 1167–1176.
Schader, A.M., Cheng, C.-Y., Israelachvili, J.N., Han, S., 2016. Communication: contrasting effects of glycerol and DMSO on lipid membrane surface hydration dynamics and forces. J. Chem. Phys. 145, 041101.
Schichman, S.A., Amey, R.L., 1971. Viscosity and local liquid structure in dimethyl sulfoxide-water mixtures. J. Chem. Phys. 75, 98–102.
Schoenborn, B.P., 1976. Neutron scattering for the analysis of membranes. Biochim. Biophys. Acta 457, 41–55.
Stumpe, M.C., Grubmüller, H., 2007. Aqueous urea solutions: structure, energetics, and urea aggregation. J. Phys. Chem. B 111, 6220–6228.
Thind, R., O'Neill, D.W., Del Regno, A., Notman, R., 2015. Ethanol induces the formation of water-permeable defects in model bilayers of skin lipids. Chem. Commun. (Camb.) 51, 5406–5409.
Trommer, H., Neubert, R.H.H., 2006. Overcoming the stratum corneum: the modulation of skin penetration. Skin Pharmacol. Physiol. 19, 106–121.
van der Merwe, D., Riviere, J.E., 2005. Comparative studies on the effects of water, ethanol and water/ethanol mixtures on chemical partitioning into porcine stratum corneum and silastic membrane. Toxicol. In Vitro 19, 69–77.
van Smeden, J., Janssens, M., Gooris, G.S., Bouwstra, J.A., 2014. The important role of stratum corneum lipids for the cutaneous barrier function. Biochim. Biophys. Acta 1841, 295–313.
Williams, A.C., 2015. Urea and derivatives as penetration enhancers. In: Dragicevic, N., Maibach, H.I. (Eds.), 2015. Percutaneous Penetration Enhancers Chemical Methods in Penetration Enhancement. Modification of the Stratum Corneum. Springer, Berlin, pp. 301–308.
Williams, A.C., Barry, B.W., 2004. Penetration enhancers. Adv. Drug Deliv. Rev. 56, 603–618.
Worcester, D.L., Franks, N.P., 1976. Structural analysis of hydrated egg lecithin and cholesterol bilayers. II. Neutron diffraction. J. Mol. Biol. 100, 359–378.
Zbytovská, J., Vavrova, K., Kiselev, M.A., Lessieur, P., Wartewig, S., Neubert, R.H.H., 2009. The effects of transdermal permeation enhancers on thermotropic phase behaviour of a stratum corneum lipid model. Colloids Surf. A Physicochem. Eng. Asp. 351, 30–37.